Journal of Oceanography, Vol. 56, pp. 173 to 183. 2000

Equatorward Spreading of a Passive Tracer with Application to North Pacific Interdecadal Temperature Variations

MASAMI NONAKA[1]*, SHANG-PING XIE[2] and KENSUKE TAKEUCHI[3]

[1]*International Pacific Research Center SOEST, University of Hawaii, Honolulu, HI 96822, U.S.A.*
[2]*Graduate School of Environmental Earth Science, Hokkaido University, Sapporo 060-0810, Japan*
[3]*Institute of Low Temperature Science, Hokkaido University, Sapporo 060-0819, Japan*

(Received 16 September 1998; in revised form 17 May 1999; accepted 29 June 1999)

A simulation is conducted with a realistic ocean general circulation model to investigate the three dimensional spreading of a passive tracer prescribed at the sea surface with the same distribution as the interdecadal sea surface temperature (SST) anomalies observed in the North Pacific. The tracers reaching the equator have the same sign as the major oval-shaped SST anomaly pattern in the central North Pacific but with a magnitude reduced less than 10% of the mid-latitude SST anomaly. The mixing both with the water containing SST anomalies of an opposite sign off the west coast of North America, and with the Southern Hemisphere thermocline water both contribute to the reduced equatorial amplitude. On the way to the equator in the southwestern part of the subtropical gyre, the subducted water is replenished by tracers leaking from the recirculation region to the north. The simulated passive tracer field in the subsurface layers agrees with the observed interdecadal temperature anomalies, suggesting the relevance of the processes studied here to the thermocline variability in the real North Pacific.

Keywords:
· North Pacific,
· interdecadal variation,
· subtropics,
· tropics,
· subduction process.

1. Introduction

Decadal/interdecadal variations in the North Pacific sea surface temperature (SST) and global atmosphere have been revealed by many studies (Nitta and Yamada, 1989; Tanimoto *et al*., 1993; Trenberth and Hurrell, 1994; Nakamura *et al*., 1997, among others). Recently, Gu and Philander (1997) and K. Hanawa (1995, personal communication) proposed a "delayed action oscillation" theory for these variations, in which the exchange of the sea water between the North Pacific and the equatorial region is a key process. In this theory, the water subducted from the North Pacific with anomalous temperatures is transported to the equatorial region on the subsurface isopycnals and then upwells to the sea surface (McCreary and Lu, 1994; Liu, 1994). The resultant equatorial SST anomalies induce anomalous atmospheric circulation that changes the sign of SST anomalies over the North Pacific. The time scale of this water migration from the subtropics to the tropics determines the time scale of this "delayed action oscillation." Recent observational studies have revealed decadal subsurface temperature anomalies (Yasuda and Hanawa, 1997) which seem to be subducted in mid-latitude and migrate southwestward along the thermocline (Deser *et al*., 1996; Schneider *et al*., 1999). However, the arrival of the North Pacific temperature anomalies at the equator via ventilation has not been demonstrated.

There are two problems with assumption of the delayed action theory that the North Pacific SST anomalies are advected into the equator intact. The first is the high potential vorticity barrier at 10°N beneath the atmospheric intertropical convergence zone (ITCZ; Xie, 1994). The subducted water with low potential vorticities may not easily pass this latitude via an interior route to the equatorial region. Instead, the water tends to go through the western boundary region (Lu and McCreary, 1995; Rothstein *et al*., 1998), where it is subjected to strong mixing and loses its characters.

The other problem with the theory arises from the relative positioning of the SST anomaly with the so-called exchange window from which the subducted water can reach the equatorial region (Liu, 1994). A large portion of the major oval-shaped decadal SST anomaly pattern in the central Pacific is not in the exchange window, while

* Corresponding author. E-mail: nona@soest.hawaii.edu

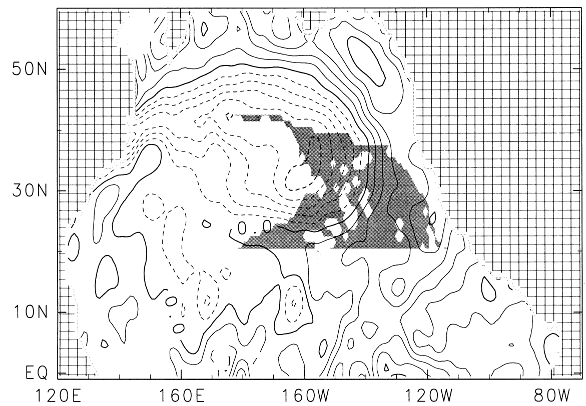

Fig. 1. Winter time (Jan.–Feb.–Mar.) SST difference between 1977–87 and 1965–75, calculated based on Comprehensive Ocean Atmosphere Data Set (COADS). Contour intervals are 0.2°C with negative value dashed. The subtropical–tropical exchange window at the bottom of the mixed layer in the model is shaded. To detect the exchange window, we compute from the annual mean velocity field the trajectories of water particles that start at all grid points from 20°N to 50°N. The exchange window is defined as the group of the starting points of these trajectories that reach the equatorial region.

the SST anomalies of the opposite sign to the east occupy about half of the exchange window (Fig. 1). Here arise two questions: Does the equatorial temperature anomaly have the same sign as the major oval-shape SST anomaly? How large is it relative to the North Pacific SST anomaly? The answer to the latter question gives a measure of the efficiency of the oceanic pipeline between the North Pacific and the equator.

Here we attempt to test the delayed action theory by using a realistic ocean general circulation model (OGCM). As a first step and as done in the delayed action theory, the equatorward spreading from the North Pacific of a passive tracer analogous to the interdecadal temperature anomaly is examined, and the tracer is advected by ocean currents but has no effect on dynamics. Thus, we neglect the complex nonlinear advection of temperature and salinity that are active tracer and affect the dynamics. This makes our problem simple and enables us to focus on the advective-diffusive effects on the three dimensional spreading of the tracer from the North Pacific by the ocean circulation. Our simplified experiment is a necessary first step toward a comprehensive treatment of temperature as an active tracer and serves as a guide for interpreting results from a more complete simulation.

The present study addresses these questions by means of a numerical simulation with an OGCM of the Pacific. We will inject the "temperature anomaly" passive tracer at the surface with the observed decadal/interdecadal SST anomaly distribution in the North Pacific and see how the tracers spread three-dimensionally into the whole Pacific.

2. Model

We use the widely used OGCM, GFDL MOM 1.1 (Pacanowski *et al*., 1991). The model covers the portion of the Pacific from 50°S to 60°N and has realistic coastline and bottom topography with the maximum depth at 5000 m. The model solves the primitive equations on a spherical coordinate, under the Boussinesq, rigid lid, and hydrodstatic approximations. The horizontal and vertical eddy viscosities are constant at 5.0×10^7 and 10.0 cm^2s^{-1}, respectively. Tracers are mixed both along isopycnal surfaces and diapycnally (Redi, 1982; Cox, 1987) with diffusivities of 2.0×10^7 and 0.3 cm^2s^{-1}, respectively. Within 5° of the model's poleward boundaries, temperature, and salinity are restored to the prescribed climatological values with seasonal variation (Levitus and Boyer, 1994; Levitus *et al*., 1994). The model employs non-slip condition and requires the fluxes of mass, temperature, and salinity to vanish at all boundaries except at the sea surface where the climatological wind stress (Hellerman and Rosenstein, 1983) is applied. Temperature and salinity are restored to the climatological value at the sea surface with a restoring time of 14 days for water of the uppermost 10-m level. Initially, the model ocean is at rest with the annual mean climatological temperature and salinity. The horizontal resolution is 1 degree, and there are 41 levels in the vertical with 10- to 15-m resolutions in the top 300 m. The model is integrated for 31 years and reaches a nearly steady state. The model result averaged for the last year is used in the following passive tracer calculation. The temperature and salinity distributions on the isopycnal surfaces in our model closely resemble those derived from the climatological data, as will be described in a separate paper (Nonaka and Takeuchi, 1999), but the structure of the model temperature field is diffused compare to the observed climatology. The current systems are reproduced quite well in our GCM, although the maximum velocities of the western boundary currents and the equatorial undercurrent are much smaller than those have been observed, deficiencies likely caused by the relatively coarse horizontal resolution of our GCM. The equatorward transports of the western boundary currents (22 Sv at 8°N, west of 130°E; 11 Sv at 3°S, west of 160°E), however, are comparable to observations (Lukas *et al*., 1991; Butt and Lindstrom, 1994). Thus the slowness of the equatorward western boundary current is not crucial for the result of this study.

To examine how the SST anomalies (Fig. 1) spread along the thermocline, the passive tracer corresponding to the temperature anomaly is injected into the model ocean by restoring its concentration at the uppermost level to the observed SST anomalies north of 20°N. The restoring time is 14 days, the same as for temperature. As we are concerned with a tropical signature of SST anomalies injected into the thermocline in the mid-latitudes, the surface tracer field is restored to zero south of 20°N. Initially, the tracer has uniformly zero field. The tracer field is in a nearly steady state after 30 years integration. The results at year 30 are analyzed.

Throughout our tracer experiments, the density stratification is fixed at its March 1 field—the time when the mixed layer is at its deepest—while annual mean velocity field is used for advection. This follows Stommel's (1979) deamon argument that only winter surface information can enter the permanent thermocline through the bottom of winter mixed layer (see also Liu and Pedlosky, 1994). This is confirmed by an additional experiment with the seasonally varying velocity and density fields. The properties of the tracer field in this case are almost the same as those of the standard case.

3. Results

Figure 2 shows the distribution of the tracer on the isopycnal surface σ_θ = 25.5 and the trajectories of water parcels starting from 30°N, 35°N, and 30°S. Negative tracers subducted at the center of the oval-shaped SST anomalies extend southwestward like a tongue to the western boundary, following the water parcel trajectories. The majority of negative tracers do not go to the tropics but recirculate within the subtropical gyre. Only tracers on the southern flank of the negative tracer tongue are advected into the equatorial region through both the interior and the western boundary exchange routes as revealed by the trajectories.

The positive tracers in high latitudes near the eastern boundary do not spread into the equatorial region on this surface. The positive tracer tongue starting from the North American coast around 25°N is likely due to the downward diffusion from the overlying layer. This positive tongue also extends southwestward, but does not reach the equator.

Figure 3 shows the tracer and density fields on the zonal sections at 30.5°N, 19.5°N. At 30.5°N, the negative tracers are centered at 160°W with a deep structure extending from the sea surface to the thermocline with east-downward tilt. The positive tracers, on the other hand, are trapped in shallow layers to the east.

Farther to the south at 19.5°N, where the tracer is restored to zero at the surface, the largest tracers of both signs are trapped in the thermocline. The core of the negative tracer moves westward and is centered on the isopycnal surface σ_θ = 25.5. The positive tracers center on shallower isopycnals σ_θ = 24.0–24.5 because they are subducted in the east where surface density is smaller than the central Pacific.

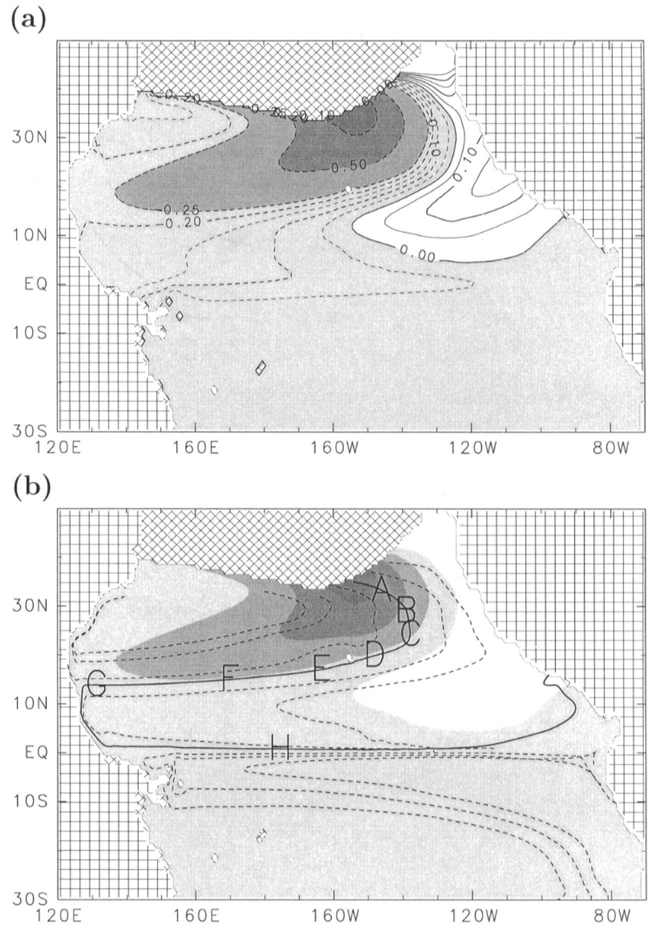

Fig. 2. (a) Tracer concentration on σ_θ = 25.5 surface. Contour intervals are 0.25, but are reduced to 0.05 for small values between –0.25 and 0.25. Negative values are dashed and shaded. (b) Trajectories of water parcels starting on the isopycnal surface σ_θ = 25.5. Shades are same as in (a). Characters A to H show the points of the water parcel moving along the trajectory with two-year intervals from year 1 to year 15.

The tracer is transported to the equator mainly through the western boundary layer where its concentration reaches a maximum at the equator (Fig. 6(a); see also Fig. 2(a)). This suggests that the western boundary route is more important for the transport of the tracers than the interior route. At the equator, the core of the negative tracer is still centered on σ_θ = 25.5 and extends eastward along the equator, riding on the strong Equatorial Undercurrent (EUC). On its way toward the east, the concentration of the tracer decreases rapidly from the western boundary. The value of the equatorial subsurface tracer concentration is less than 20% of the maximum SST anomalies prescribed over the North Pacific. East of

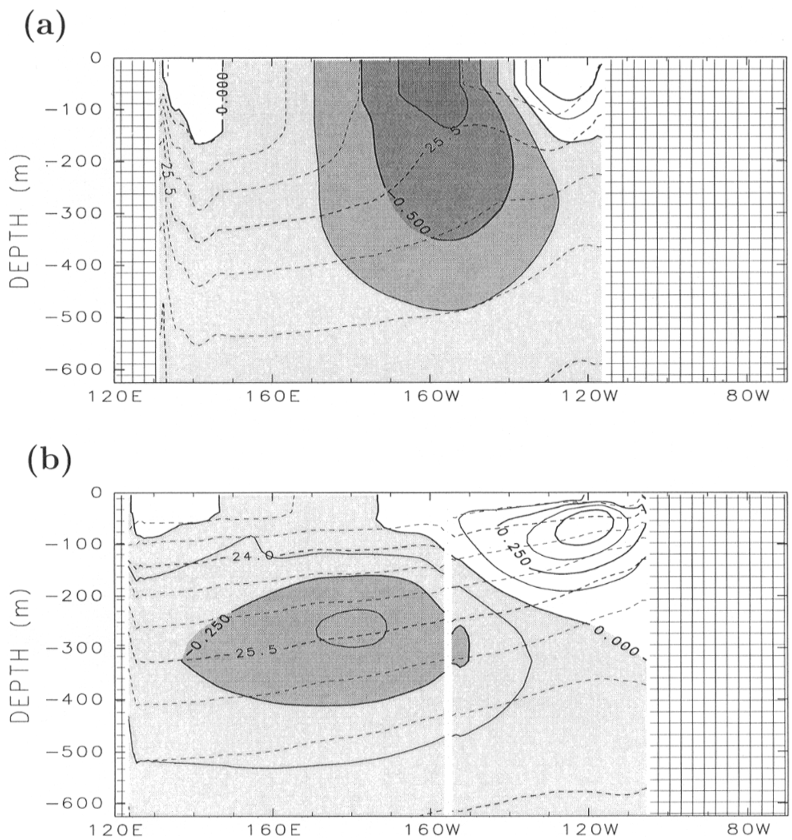

Fig. 3. Tracer concentration (solid) and density (dashed line) on zonal sections at (a) 30.5, (b) 19.5°N. Negative tracer values are shaded. Contour intervals are 0.125 at 19.5°N, 0.25 at 30.5°N, and 0.50 for σ_θ.

160°E, the ratio of equatorial tracers to mid-latitude anomalies is less than 10%.

4. Roles of Diffusion

4.1 Steady state

The tracer transported from the North Pacific is strongly affected by the diffusion on the way to the equator. While the diapycnal mixing simply diffuses the tracer (Fig. 5), the isopycnal diffusion affects the tracer advected into the equatorial region in some interesting ways. To illustrate this, we show the tracer concentration (Fig. 4) and the tracer balance budget (Fig. 5) along a trajectory linking the North Pacific to the equator. On this trajectory, the negative tracer subducted from the large SST anomaly region in the exchange window is advected southeastward and then southwestward. However, these subducted signals decay rapidly (from point A to D) because of isopycnal mixing (Fig. 5(a)). Within the exchange window, the SST anomalies change signs (Fig. 1) and contain a strong horizontal gradient. The tracers of opposite signs mix with and offset each other on the long way to the tropics and the positive value of the tracer does not extend to the equator (Fig. 2(a)). The small equatorial tracer concentration is mainly caused by this rapid decay just after the subduction.

The second major isopycnal mixing event takes place in a narrow band in the southwestern part of the subtropical gyre. As shown in Fig. 2(b), the trajectories of water parcels that are widely separated at 30°N gradually converge meridionally as they move to the south. The potential vorticity barrier mentioned in the introduction prevents the trajectories from entering the tropics through the interior region and forces them to stack up near 10°N. This intensifies the isopycnal diffusion (Fig. 5). Part of the recirculating negative tracers in the subtropical tongue are thus diffused toward the south, and the water going to the equator is replenished with negative tracers, as indicated by an increase in the negative concentration in Fig. 4 from point D to F. In the real ocean, baroclinic eddies are the likely agents of mixing tracers across mean flow trajectories. High eddy activity is observed by satellite altimetry along 20°N over the southwestern subtropical gyre (Fu and Smith, 1996), where the meridional gradi-

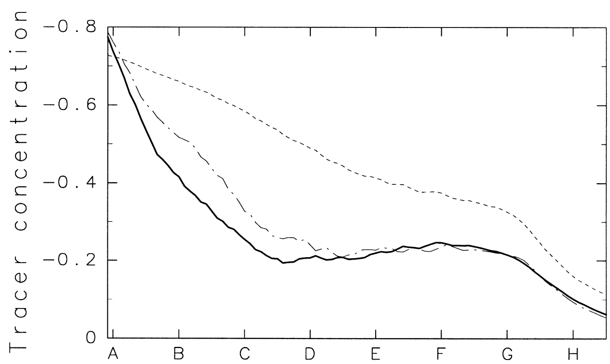

Fig. 4. Tracer concentration on the trajectory (solid line with characters in Fig. 2(b)) for the standard experiment (solid), for the zonally uniform SST anomaly experiment (dashed line), and for the weak isopycnal mixing experiment (dash-dotted line).

ent of potential vorticity changes sign in the vertical (Talley, 1988), a necessary condition for baroclinic instability (Gill *et al.*, 1974).

The rapid decay near the western boundary at the equator (Fig. 2(a); Fig. 6(a)) is due to the Southern Hemisphere water, with almost zero tracer value in our experiments. It is transported into the equatorial region through both the interior and the western boundary route (Fig. 2(b)). This western boundary current is known as the New Guinea Coastal Undercurrent (NGCUC; Lindstrom *et al.*, 1987). In our model, the NGCUC joins the EUC around 150°E, diluting the Northern Hemisphere tracer. The mixing with the Southern Hemisphere water that enters the equator through the interior route further contributes to the gradual eastward decrease of the negative tracers east of 160°E (Fig. 6(a)).

The tracers subducted in the North Pacific are also subjected to vertical diffusion on the way into the Tropics (Fig. 5(a)). As the negative tracer is subducted only in a limited range of latitudes, the subducted water forms a relatively thin layer, of only a few hundred meters thick (Fig. 3). The conservation of potential vorticity requires the layer to become even thinner as it approaches the tropics, increasing vertical diffusion. Along the equator, the vertical mixing along with upwelling brings the tracers to the surface.

Because the sea surface tracer distribution affects gradient on isopycnals and hence relative importance of mixing, the important roles of mixing shown here suggest that the tracer field on an isopycnal is affected by the sea surface distribution. For example, the rapid decay in the negative tracer concentration just after the subduction (Fig. 4, from point A to C) is due to the isopycnal mixing with the positive tracer to the east. To examine the effect of this eastern positive tracer, we perform another experiment where the sea surface tracers are restored to the zonally uniform field with a meridional distribution obtained by averaging the observed SST anomaly field (Fig. 1) from 170°E to 150°W, eliminating the eastern positive tracer at the sea surface. The design of this experiment is perhaps more in line with the concept of the simple delayed action theory. Removing the positive tracers off the west coast of North America substantially reduces the isopycnal diffusion just after the subduction (Fig. 5(b), from point A to D), and as a result, the decay rate of the subducted negative tracer decreases to about third of that in the standard case (Fig. 4, dashed line).

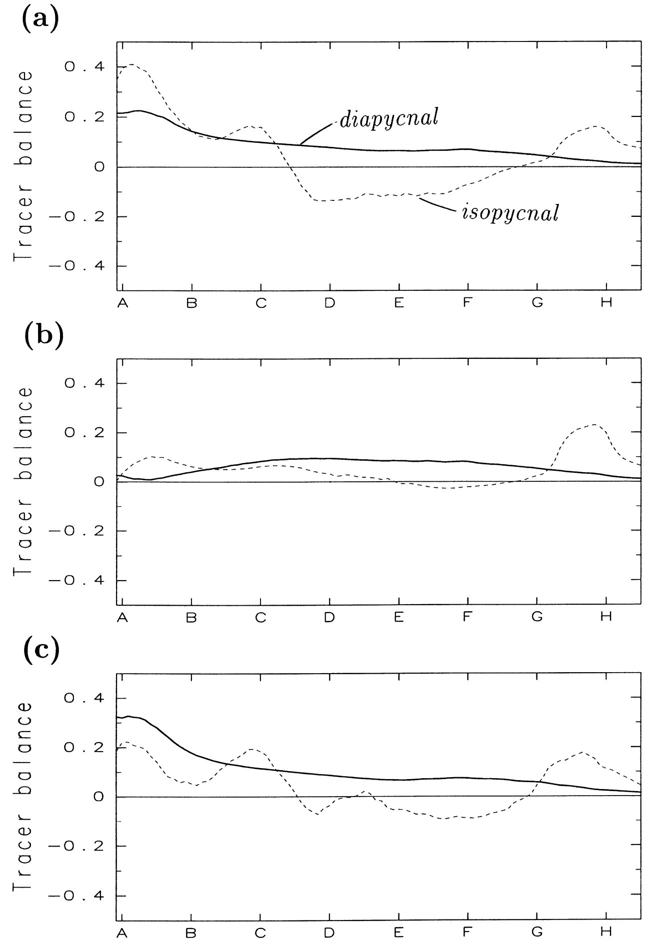

Fig. 5. (a) Tracer balance budget on the same trajectory as Fig. 4 at year 30. (b) Same as (a) except for the zonally uniform SST anomaly experiment. (c) Same as (a) except for the weak isopycnal mixing experiment. The solid (dashed) line shows the diapycnal (isopycnal) mixing. These figures show the tracer budget balance on a Lagrangian particle. Thus, even in the steady state, the sum of the tracer budget is not zero and the net decrease of the tracer concentration on a water particle equals the sum of the isopycnal and diapycnal diffusions in the steady state.

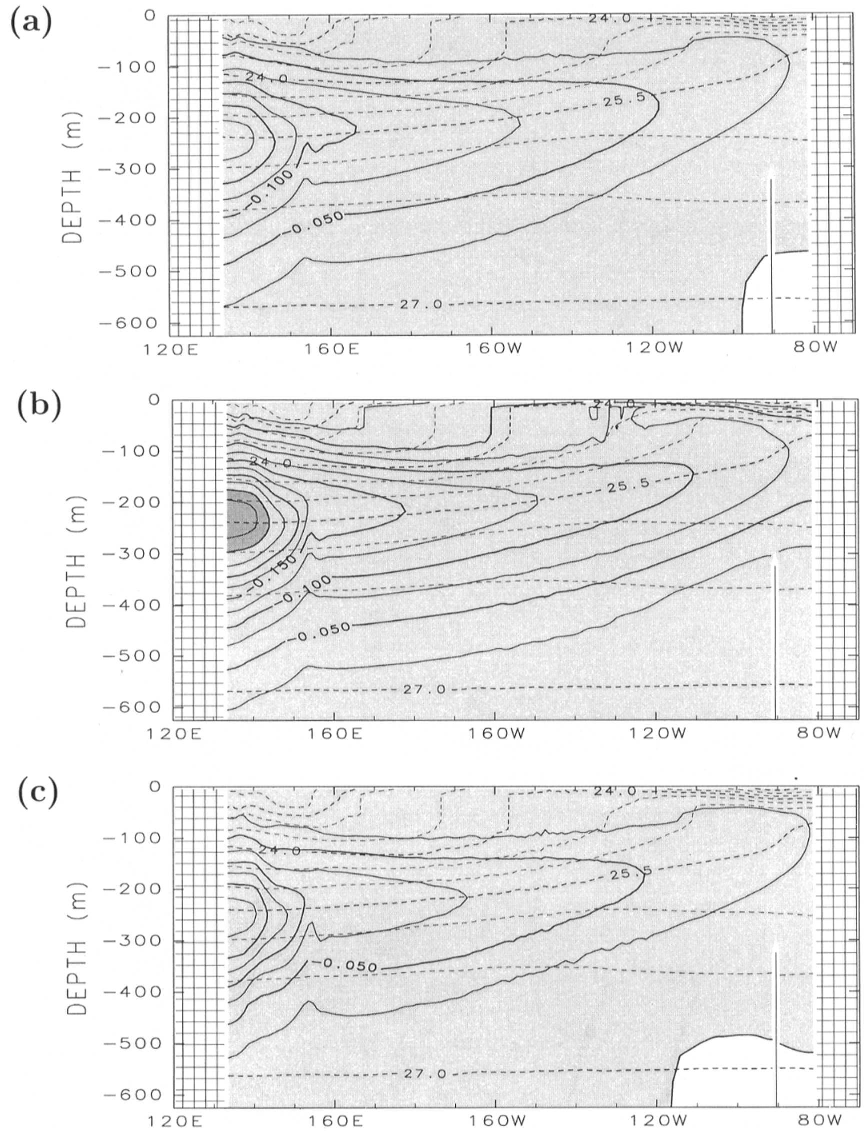

Fig. 6. Tracer concentration (solid) and density (dashed line) on zonal sections at the equator for (a) the standard case, (b) the zonally uniform SST anomaly experiment and (c) the small isopycnal mixing case. Negative tracer values are shaded. Contour intervals are 0.025 for tracer and 0.50 for σ_θ.

The zonally uniform sea surface tracer field also reduces the horizontal gradient in the southwestern part of the subtropical gyre. This weakens the isopycnal diffusion and hence the replenishment from the recirculation region (Fig. 5(b), from point D to F). With this weak replenishment, the tracer concentration of the water particle decreases continuously due to the diapycnal mixing (Fig. 4, dashed line). As a result, the weaker horizontal gradient and reduced isopycnal mixing increase the equatorial tracer concentration by a factor of two (Fig. 6(b)), demonstrating the importance of the subtropical sea surface distribution of the tracer on the equatorial tracer concentration.

Because of the importance of the isopycnal mixing shown here, our results may have a dependence on the magnitude of the coefficient of the diffusion. To examine this, we perform a sensitivity experiment with an isopycnal diffusivity reduced to one half, 1.0×10^7 cm^2s^{-1}. The procedures to make the annual mean velocity field and to perform the tracer experiment are the same as in the standard case. The tracer concentration on the trajectory followed from the same point as in the standard case shows that the first rapid decay (Fig. 4, from A to D of dash-dotted line) associated with the mixing with

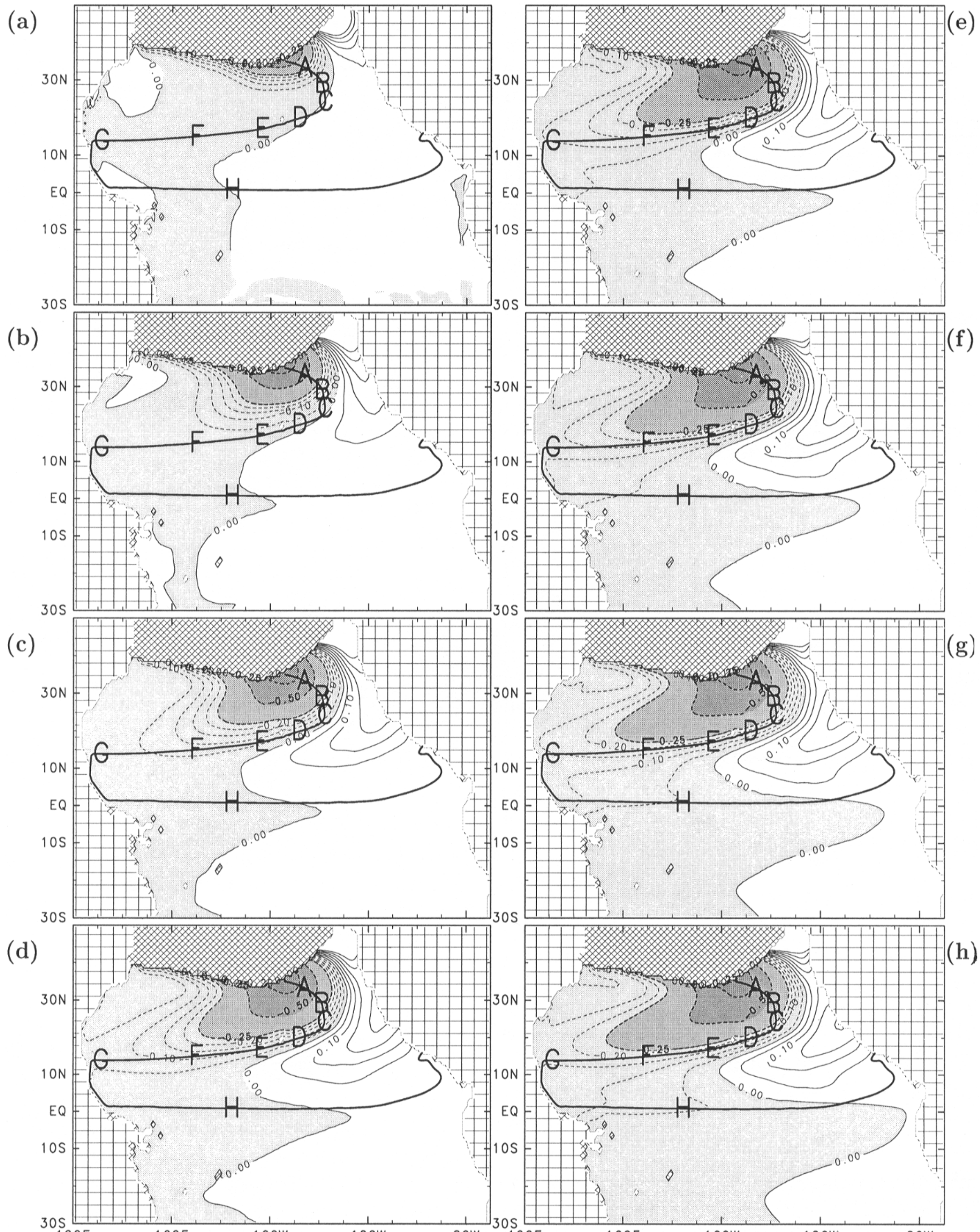

Fig. 7. Tracer concentration on σ_θ = 25.5 surface at year 1 (a) and year 15 (h). Each panel is two years apart with the next. Contour intervals are 0.05 for –0.25 to 0.25. Negative values are dashed and shaded.

positive tracers to the east weakens (Fig. 5(c)). Meanwhile, the leakage from the recirculation around point F is also reduced (Figs. 4 and 5(c)). These two effects of the weak isopycnal mixing compensate each other and make the tracer concentration at the equatorial region almost the same as in the standard case (Fig. 4; Fig. 6(c)). These results show that although the tracer concentration on the way from the North Pacific to the equator depends on the size of the isopycnal mixing, at the equatorial region the tracer concentration is not so sensitive to the size of the mixing coefficient. In this weak isopycnal mixing case, the negative tracer concentration increases only slightly around point F. Nevertheless, the replenishment via the isopycnal mixing does happen (Fig. 5(c)). Even in the zonally uniform sea surface tracer case, although the tracer concentration continues to decrease around point F (Fig. 4, dashed line), a weak replenishment appears in the tracer balance (Fig. 5(b)) to reduce the rate of decrease in tracer concentration. Thus, the replenishment from the recirculation region happens in all these cases with the effect of increasing the tracer concentration in the equatorial region.

4.2 Transient variation

The period of the "delayed action oscillation" is determined by the time scale to transport the temperature anomaly from the North Pacific to the equator (Gu and Philander, 1997). In addition to a purely advective time scale determined by current velocity only, the isopycnal mixing introduces other time scales as well. Here, we will investigate these time scales by examining the transient time development of the tracer field and seeing how tracers injected into the North Pacific spread to the equatorial region.

Figure 7 shows how the tracer field on the isopycnal surface $\sigma_\theta = 25.5$ varies with time from the initial condition of zero tracer value in the whole ocean. The front of the subducted tracer moves southwestward toward the western boundary and then the southern branch bifurcates moving southward to the equator along the western boundary.

To show the movement of this subducted tracer front, we plot the time-distance development of the time derivative of the tracer concentration along the trajectory shown in Fig. 7 (Fig. 8). The vertical axis of this figure shows the years after the injection of the tracer at the sea surface and the horizontal axis is the along-the-trajectory distance. It is so arranged that it takes two years for a water parcel on the trajectory to move from one alphabetic character to the next. The straight lines in the figure thus indicate the paths that a water parcel follows.

The front of the tracer subducted from the sea surface moves with the water parcel, along the straight line, from point A and decays rapidly up to point D. The time scale of this subducted water parcel to arrive at the equatorial region is about 15 years, after which the tracer field approaches a steady state. A remarkable feature of Fig. 8 is a sudden rapid increase in tracer concentration around year 5, point F. This concentration front is then advected to the equatorial region. It is this tracer that first arrives at the equatorial region around year 10, well before the water parcel advected from point A does.

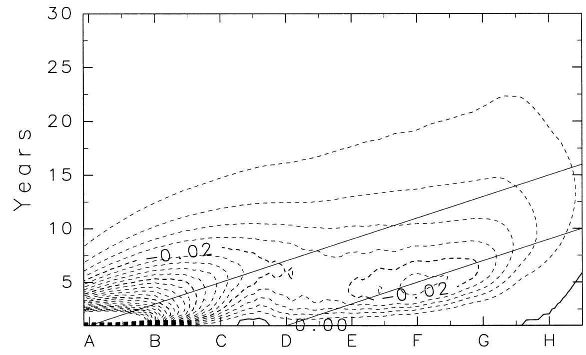

Fig. 8. Time derivative of tracer concentration as a function of distance and time on the trajectory shown in Fig. 7. The horizontal axis is so arranged that a water parcel's trajectory appears as a straight line in the figure. It takes two years for a water parcel to move from one alphabetic character to the next. Contour intervals are 0.004°C year^{-1}.

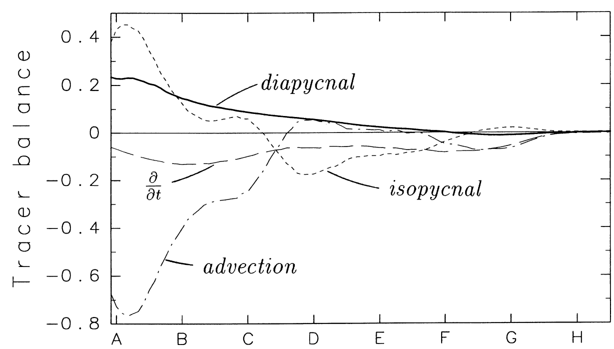

Fig. 9. Same as Fig. 5, but at year 5 after the inject of the tracer from the sea surface. The dashed–dotted (long-dashed) line shows the advection (time derivative).

Then, what supplies this tracer that arrives first at the equatorial region? The tracer balance at year 5 on the same trajectory (Fig. 9) confirms that it is the isopycnal mixing (Fig. 9, dashed line) that supplies the tracer around point F and makes the rapid increase that appeared in Fig. 8, the same replenishment shown in the steady state solution. At year 5, although the tracer subducted from the sea surface within the exchange window is advected to only around point C (Fig. 8, straight line from point A; Fig. 9, dash-dotted line), the recirculating negative tracer tongue has moved to the north of the points E and F (Fig. 7(c)). The negative tracer of this tongue is mixed isopycnally onto the trajectory that leads eventually to the equatorial region. Thus, the isopycnal mixing in the southwestern part of the subtropics replenishes the tracer around point F before the tracer advected along this trajectory arrives and provides a short cut to the equatorial region, reducing the journey from the North Pacific to the equator by 5 years compared with a purely advective route.

5. Discussion and Conclusion

In a realistic OGCM, the equatorward spreading of the tracer corresponding to the North Pacific decadal/interdecadal SST anomaly through the subduction-ventilation process has been examined. Here, we compare the simulated passive tracer fields with the observed interdecadal temperature anomalies. The meridional section of the tracer at 30.5°N (Fig. 3(a)) shows the eastern shallow positive tracers and the central deep negative tracers tilting east-downward, reminiscent of the observed temperature difference between the decades of 1976–85 and 1966–75 (Yasuda and Hanawa, 1997). At 19.5°N where tracer is restored to zero at the surface, the negative tracers submerge into the subsurface and move southwestward with the core staying around $\sigma_\theta = 25.5$ (Fig. 3(b)), an isopycnal surface on which Deser *et al*. (1996) observed the migration of the negative temperature anomaly core during 1977–1991. Zhang *et al*. (1998) analyzed historical temperature data and showed the migration of the temperature anomaly from the North Pacific to the equatorial region. More recently, Schneider *et al*. (1999) showed that the migration from 18°N to the equatorial region is locally forced, although the southwestward migration from the central North Pacific can be followed to 18°N of the western boundary.

These results are consistent with our results that the subducted tracer migrates southwestward and the majority of the negative tracer does not go into the tropics but recirculates within the subtropics (Figs. 2(a) and 7). The results of Schneider *et al*. (1999) also showed that the eastern anomalies off the North America do not reach the equatorial region and the central anomalies decay rapidly during the southwestward migration, suggesting the importance of the mixing emphasized in this study.

These similarities between the simulated passive tracer field and the observed interdecadal temperature anomalies suggest that the processes of the equatorward spreading of the passive tracers examined in this study are relevant and can help understand the migration of the North Pacific temperature anomalies.

In this study, we have examined the equatorward spreading of the tracer injected into the ocean steadily. The SST field in the North Pacific, however, has variations on various time scales (Tanimoto *et al*., 1993). Thus it is important to take into account the effect of the temporal variations at the sea surface. In an experiment where the surface tracer field varies on an interdecadal time scale, the leak from the recirculation onto an equator-going trajectory in the southwestern part of the subtropics is important, much as in the standard case (not shown). When the sea surface tracer varies at a period of twenty years—a period seen in the variation of the sea level pressure in the North Pacific (e.g. Minobe, 1999)—this replenishment from the recirculating tracers becomes even more important, supplying most of the tracer that reaches the equator.

The tracer corresponding to the North Pacific interdecadal SST anomaly reaches the equator and, as hypothesized in the delayed action theory, the tracer has the same sign at the equator as the SST anomalies in the major oval-shaped pattern occupying most of the North Pacific but with a much reduced magnitude. Our simulation reveals that the majority of the SST anomalies do not reach the tropics and isopycnal mixing is an important process in the water exchange problem between the North Pacific and the equator.

Here we summarize our results, by following a water parcel on the trajectory shown in Fig. 4:

a) The subducted water with negative tracers is subjected to strong mixing with positive tracers to the east;

b) In the southwestern part of the subtropical gyre, the water is replenished with negative tracers leaked from the recirculation region to the north;

c) The water particle enters the equator through the western boundary region; and

d) The negative tracers are substantially diluted by the intrusion of the Southern Hemisphere thermocline water and the remnants are carried eastward by the EUC along the equator.

Conclusion a) spotlights the importance of SST distribution: the positive SST anomaly region near the eastern boundary, which has been somewhat overlooked in literature, affects the magnitude of the equatorial tracers. Conclusion d) is only tentative as a lack of data prevented us from obtaining decadal SST anomalies over the South Pacific. If mid-latitude SST anomalies over the North and South Pacific are in phase with each other, the blending of the water from the two hemispheres will enhance the equatorial temperature anomalies. Because the volume transport of the water from the subtropics to the equatorial region in the Southern Hemisphere (11.7 Sv at 15°S) is comparable to that in the Northern Hemisphere (20.6 Sv at 15°N), the influence of the Southern Hemisphere to the equatorial tracer field could be as important as that of the Northern Hemisphere, although it depends on the sea surface distribution of sea surface tracer. Thus, it is very important to investigate the influence of the Southern Hemisphere; however, we cannot execute the experiment to investigate it, because unfortunately we have not enough data to detect the interdecadal temperature anomaly fields at the sea surface and in the subsurface in the Southern Hemisphere, which are needed to give the sea surface boundary condition and to confirm the validity of the model results.

As shown in Fig. 8, the leakage of the recirculating subtropical tracers onto an equatorward pathway provides a short cut to the equatorial region. As a result, the shorter time scale of the equatorward spreading of the North Pacific tracers than the pure advection time scale is established.

This study has focused on the problem of how North Pacific interdecadal SST anomalies would spread as a passive tracer into the thermocline and to the equator. In the reality, the interdecadal temperature anomaly makes the density anomaly about $0.3\sigma_\theta$, thus its core would appear around a different isopycnal surface, and this anomaly would propagate as internal waves through the thermocline. Most recent theoretical studies (Liu, 1999; A. Kubokawa and M. Nagakura, 1999, personal communication) showed that a temperature anomaly subducted into the thermocline forces waves that propagate on the thermocline in the direction of the isopycnal velocity, albeit at a speed slower than the advection velocity. Therefore, the active temperature anomalies would propagate more slowly than those in this study. We are currently investigating the spreading of the temperature anomalies as an active tracer. The three-dimensional variations in ocean temperature become a more complicated problem when we take into account wind forcing variation. The SST anomalies shown in Fig. 1 are caused by anomalous winds in the first place (Trenberth and Hurrell, 1994), and these anomalous winds have further effects on ocean currents and thermocline depth distribution. To assess these dynamic effects, future studies that treat temperature as a dynamically active tracer under realistic wind variations are needed.

Acknowledgements

We thank Drs. A. Kubokawa, Y. Yamanaka and J. P. McCreary for their invaluable comments and encouragements. This study is supported by grants from Frontier Research System for Global Change and University of Tokyo's Center for Climate System Research. The figures were produced by GFD-DENNOU library. SOEST contribution number 4862. IPRC contribution number 15.

References

Butt, J. and E. Lindstrom (1994): Currents off the east coast of New Ireland, Papua New Guinea, and their relevance to regional undercurrents in the Western Equatorial Pacific Ocean. *J. Geophys. Res.*, **99**, 12503–12514.

Cox, M. D. (1987): Isopycnal diffusion in a *z*-coordinate ocean model. *Ocean Modeling*, **74**, 1–5.

Deser, C., M. A. Alexander and M. S. Timlin (1996): Upper-ocean thermal variations in the North Pacific during 1970–1991. *J. Climate*, **9**, 1840–1855.

Fu, L.-L. and R. D. Smith (1996): Global ocean circulation from satellite altimetry and high-resolution computer simulation. *Bull. Amer. Meteor. Soc.*, **77**, 2625–2636.

Gill, A. E., J. S. A. Green and A. J. Simmons (1974): Energy partition in the large-scale ocean circulation and the production of mid-ocean eddies. *Deep-Sea Res.*, **21**, 499–528.

Gu, D. and S. G. H. Philander (1997): Interdecadal climate fluctuations that depend on exchanges between the tropics and extratropics. *Science*, **275**, 805–807.

Hellerman, S. and M. Rosenstein (1983): Normal monthly wind stress over the world ocean with error estimates. *J. Phys. Oceanogr.*, **13**, 1093–1104.

Levitus, S. and T. P. Boyer (1994): World Ocean Atlas 1994, Vol. 4, Temperature. NOAA Atlas NESDIS 3, 117 pp., U.S. Dep. of Commer., Washington, D.C.

Levitus, S., R. Burgett and T. P. Boyer (1994): World Ocean Atlas 1994, Vol. 3, Salinity. NOAA Atlas NESDIS 3, 97 pp., U.S. Dep. of Commer., Washington, D.C.

Lindstrom, E., R. Lukas, R. Fine, E. Firing, S. Godfrey, G. Meyers and M. Tsuchiya (1987): The western equatorial Pacific Ocean circulation study. *Nature*, **330**, 533–537.

Liu, Z. (1994): A Simple model of the mass exchange between the subtropical and tropical ocean. *J. Phys. Oceanogr.*, **24**, 1153–1165.

Liu, Z. (1999): Forced planetary wave response in a thermocline gyre. *J. Phys. Oceanogr.*, **29**, 1036–1055.

Liu, Z. and J. Pedlosky (1994): Themocline forced by annual and decadal surface temperature variation. *J. Phys. Oceanogr.*, **24**, 587–608.

Lu, P. and J. P. McCreary (1995): Influence of the ITCZ on the flow of the thermocline water from the subtropical to the equatorial Pacific Ocean. *J. Phys. Oceanogr.*, **25**, 3076–3088.

Lukas, R., E. Firing, P. Hacker, P. Richardson, C. Collins, R. Fine and R. Gammon (1991): Observations of the Mindanao Current during the western Equatorial Pacific Ocean circulation study. *J. Geophys. Res.*, **96**, 7089–7104.

McCreary, J. P. and P. Lu (1994): Interaction between the subtropical and equatorial ocean circulations: The subtropical cell. *J. Phys. Oceanogr.*, **24**, 466–497.

Minobe, S. (1999): Resonance in bidecadal and pentadecadal climate oscillaions over the North Pacific: Role in climatic regime shifts. *Geophs. Res. Lett.*, **26**, 855–858.

Nakamura, H., G. Lin and T. Yamagata (1997): Decadal climate variability in the North Pacific during the recent decades. *Bull. Amer. Meteor. Soc.*, **78**, 2215–2225.

Nitta, T. and S. Yamada (1989): Recent warming of tropical sea surface temperature and its relationship to the northern hemisphere circulation. *J. Meteor. Soc. Japan*, **67**, 375–383.

Nonaka, M. and K. Takeuchi (1999): Tropical subsurface salinity and tritium distribution in a Pacific GCM: Their differences and formation mechanisms (in preparation).

Pacanowski, R. C., K. W. Dixon and A. Rosati (1991): The GFDL Modular Ocean Model Users Guide. GFDL Ocean Group Tech. Rep. No. 2.

Redi, M. (1982): Oceanic isopycnal mixing by coordinate rotation. *J. Phys. Oceanogr.*, **12**, 1154–1158.

Rothstein, L. M., R.-H. Zhang, A. J. Busalacchi and D. Chen (1998): A numerical simulation of the mean water pathways in the subtropical and tropical Pacific Ocean. *J. Phys. Oceanogr.*, **28**, 322–342.

Schneider, N., A. J. Miller, M. A. Alexander and C. Deser (1999): Subduction of decadal North Pacific temperature anomalies: Observations and dynamics. *J. Phys. Oceanogr.*, **29**, 1056–1070.

Stommel, H. (1979): Determination of water mass properties of water pumped down from the Ekman layer to the geostrophic flow below. *Proc. Natl. Acad. Sci. USA*, **76**, 3051–3055.

Talley, L. D. (1988): Potential vorticity distribution in the North Pacific. *J. Phys. Oceanogr.*, **18**, 89–106.

Tanimoto, Y., N. Iwasaka, K. Hanawa and Y. Toba (1993): Characteristic variations of sea surface temperature with multiple time scales in the North Pacific. *J. Climate*, **6**, 1153–1160.

Trenberth, K. E. and J. W. Hurrell (1994): Decadal atmosphere–ocean variations in the Pacific. *Climate Dyn.*, **9**, 303–319.

Xie, S.-P. (1994): Oceanic response to the wind forcing associated with the Intertropical Convergence Zone in the northern hemisphere. *J. Geophys. Res.*, **99**, 20393–20402.

Yasuda, T. and K. Hanawa (1997): Decadal changes in the mode water in the midlatitude North Pacific. *J. Phys. Oceanogr.*, **27**, 858–870.

Zhang, R.-H., L. M. Rothstein and A. J. Busalacchi (1998): Origin of warming and El Nino change on decadal scales in the tropical Pacific Ocean. *Nature*, **391**, 879–883.